J Mater Sci: Mater Electron (2017) 28:9265–9271
DOI 10.1007/s10854-017-6662-7

Characterization and electrical conductivity of $La_{1-x}Sr_xCrO_3$ NTC ceramics

Ping Luo[1,2] · Bo Zhang[2] · Qing Zhao[2] · Donglin He[2] · Aimin Chang[2]

Received: 23 December 2016 / Accepted: 25 February 2017 / Published online: 15 March 2017

Abstract The $La_{1-x}Sr_xCrO_3$ (x = 0–0.1) negative temperature coefficient (NTC) ceramics have been prepared by the traditional solid state reaction method. X-ray diffraction (XRD) analysis has revealed that the as-sintered ceramics crystallize in a single perovskite structure. Scanning Electron Microscope (SEM) images show that the doped Sr^{2+} contributes to in the decrease in porosity. X-ray photoelectron spectroscopy (XPS) analysis indicates the existence of Cr^{3+} and Cr^{6+} ions on lattice sites, which result in hopping conduction. The presence of the Cr^{6+} is one of the key factors that affect the electrical conductivity of $La_{1-x}Sr_xCrO_3$. Resistance–temperature characteristics were studied in the range of −80 to 10 °C for the ceramic samples, the electrical characterizations show that the electrical resistivity and material constant B decrease with the increase of the strontium content.

1 Introduction

$LaCrO_3$ material is stable perovskite rare earth oxide having attracted extensive attention of researchers because of their variety of properties, such as good conductivity, excellent catalytic performance, outstanding ferroelectric and etc. [1–5]. $LaCrO_3$ material by doping other metallic elements in A or B-sites get rapid development owing to their excellent properties, such as high melting points, high mechanical, chemical stability and good electrical conductivity [6–8]. Furthermore, $LaCrO_3$ doped with appropriate impurity ions can be applied to the NTC thermistor materials [9, 10]. NTC thermistors are thermally sensitive resistors whose resistance decreases with increasing temperature [11, 12]. However, $LaCrO_3$ material has too high electrical resistivity at room temperature because of the weak sintering properties in the air. In order to improve the electrical properties of $LaCrO_3$, the A-site was doped by alkaline-earth metals [13, 14]. Considering the ions radius of Sr^{2+} and La^{3+} is similar, and the introduction of Sr^{2+} into the lattice could be compensated by the oxidation from Cr^{3+} to Cr^{6+} [15, 16], the substitution of Sr^{2+} for La^{3+} in $LaCrO_3$ will promote the hopping conductivity due to the presence of Cr^{3+} and Cr^{6+} ions and thereby decrease resistivity [15, 17]. Therefore, it is possible that NTC thermistor material could be obtained through the substitution of Sr^{2+} for La^{3+} in $LaCrO_3$. In this paper, the new NTC ceramic material $La_{1-x}Sr_xCrO_3$ (x = 0–0.1) were studied. The structure and electrical properties of $La_{1-x}Sr_xCrO_3$ (x = 0–0.1) ceramics were investigated.

2 Experimental procedures

Powders of $La_{1-x}Sr_xCrO_3$ (x = 0–0.1) were prepared by solid-state reaction. Stoichiometric amounts of La_2O_3 (purity >99.99%, Sinopharm Chemical Reagent co., Ltd, China), Cr_2O_3 (purity >99%, Sinopharm Chemical Reagent co., Ltd, China), and $SrCO_3$ (purity >99%, Sinopharm Chemical Reagent co., Ltd, China) were well mixed,

✉ Qing Zhao
13999994071@163.com

✉ Aimin Chang
changam@ms.xjb.ac.cn

[1] School of Physics Science and Technology, Xinjiang University, Urumqi 830046, China

[2] Key Laboratory of Functional Materials and Devices for Special Environments of CAS, Xinjiang Key Laboratory of Electronic Information Materials and Devices, Xinjiang Technical Institute of Physics & Chemistry of CAS, Urumqi 830011, China

ground, and calcined at 1100 °C for 5 h. The calcined powders were then milled in mortar for 8 h. Subsequently, the powders were pressed at 10 MPa to form a disk of 10 mm in diameters and 3 mm in thickness, and then cold isostatic pressing at 150 MPa was used to enhance densities. The pressed disks were sintered in the temperature of 1600 °C for 5 h.

X-ray diffraction (XRD; BRUKERD8-ADVANCE, Cu K_α radiation) analysis was used to identify the crystalline phases of the sintered ceramic samples. Scanning Electron Microscope (SEM; Zeiss SUPRA 55 VP, Germany) was used to observe the microstructure of the sintered ceramic samples. X-ray photoelectron spectroscopy (XPS; Thermo, ESCALAB 250XI) was used to analyze the chemical states of the sintered ceramics.

In order to obtain the electrical conductivity, the disks were coated with a platinum paste, and then annealed at 1200 °C for 2 h. The resistivity was measured in the temperature of −80 to 10 °C by Agilent34970A multimeter in an oil bath.

3 Results and discussion

Figure 1 shows the XRD patterns of the as-sintered $La_{1-x}Sr_xCrO_3$ ceramics. Analysis of these diffractograms has revealed that the ceramics are indexed to be orthorhombic perovskite phase isomorphic to $LaCrO_3$ (32-1240 card) described by the space group is P bmn. There is no other impurity phase, which shows that Sr^{2+} has all entered the perovskite lattice to form the solid solution. It is noted that the peaks corresponding to the perovskite phase in the ceramic samples slightly shift toward higher angles with the increase of Sr^{2+}, which means that the unit cell volume decreases. This result from many factors such as the ionic radius of the acceptor dopant (Sr^{2+}), the mixed valence state of the chromium ion, and the oxygen deficiency. The substitution of size larger Sr^{2+} (0.144 nm) for La^{3+} (0.136 nm) should cause an incremental increase in the until cell volume. However, the crystal structure cell volume decreased with the increase of Sr^{2+}. Comparing the sizes of the relevant ions, it is clear that the amount of the relative increment in the unit cell volume due to the substitution of larger Sr is less than that of the relative decrement caused by the formation of chrome ions, which leads to the lattice contraction. $La_{1-x}Sr_xCrO_3$ ceramics introduction of Sr^{2+} contributes to the Cr^{3+} was oxidized to Cr^{6+}, which results in the decrease in the cell volume as a result of Cr^{6+} (0.044 nm) radius less than Cr^{3+} (0.055 nm). The results will be discussed with XPS analysis.

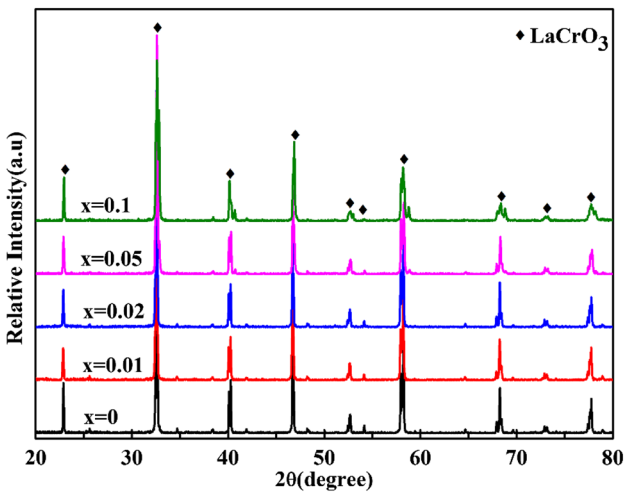

Fig. 1 XRD patterns of as-sintered $La_{1-x}Sr_xCrO_3$ ceramics

Figure 2 shows the SEM micrographs of the as-sintered $La_{1-x}Sr_xCrO_3$ ceramics. As can be seen, there was high porosity on the surface of ceramics, and the size of agglomerate Sr^{2+} doped $LaCrO_3$ samples slightly decreases compared to pure $LaCrO_3$. This may be due to the chromium volatilization at the high temperature in air atmosphere [15, 18]. Therefore, the chromium vaporization will be results in a poor sinterability of these ceramics and thereby producing little pore.

Figure 3 shows the XPS spectra of La 3*d* obtained from the ceramic samples. It can be seen that the spectra peaks are associated with the presence of lanthanum in the form of La^{3+} [19]. Figure 4 shows XPS spectra of Sr 3*d* obtained from the ceramic samples. It can be seen that the spectra only contained one single peak associated with the presence of strontium in the form of Sr^{2+} [20].

Figure 5 shows the XPS spectra and the curve-fitting example of $La_{1-x}Sr_xCrO_3$ ceramics in the regions of Cr 2*p* core-level peaks. As can be seen, the peaks in the Cr 2p3/2 and Cr 2p1/2 spectra can be split into two peaks. The peak at 576.0 eV is assigned to Cr^{3+} and 580.0 eV to Cr^{6+} [21]. Similar result has been reported on other doped lanthanum chromite systems [13, 21]. From Fig. 5, it can be seen that Cr^{6+} concentration increases with increasing Sr concentration, which lead to decreasing the cell volume. This is agreement with the previous XRD results.

Figure 6 shows the relationship between the natural logarithm of the resistivity (In ρ) and the reciprocal of the absolute temperature (1000/T) for the as-sintered $La_{1-x}Sr_xCrO_3$ NTC thermistors. It can be seen that the samples exhibited typical NTC characteristic whose resistivity decreases with increasing temperature over the measured temperature range. The resistance of NTC thermistors can be expressed by the equation [22, 23]:

$$\rho = \rho_0 \exp\left(\frac{E_a}{KT}\right) \quad (1)$$

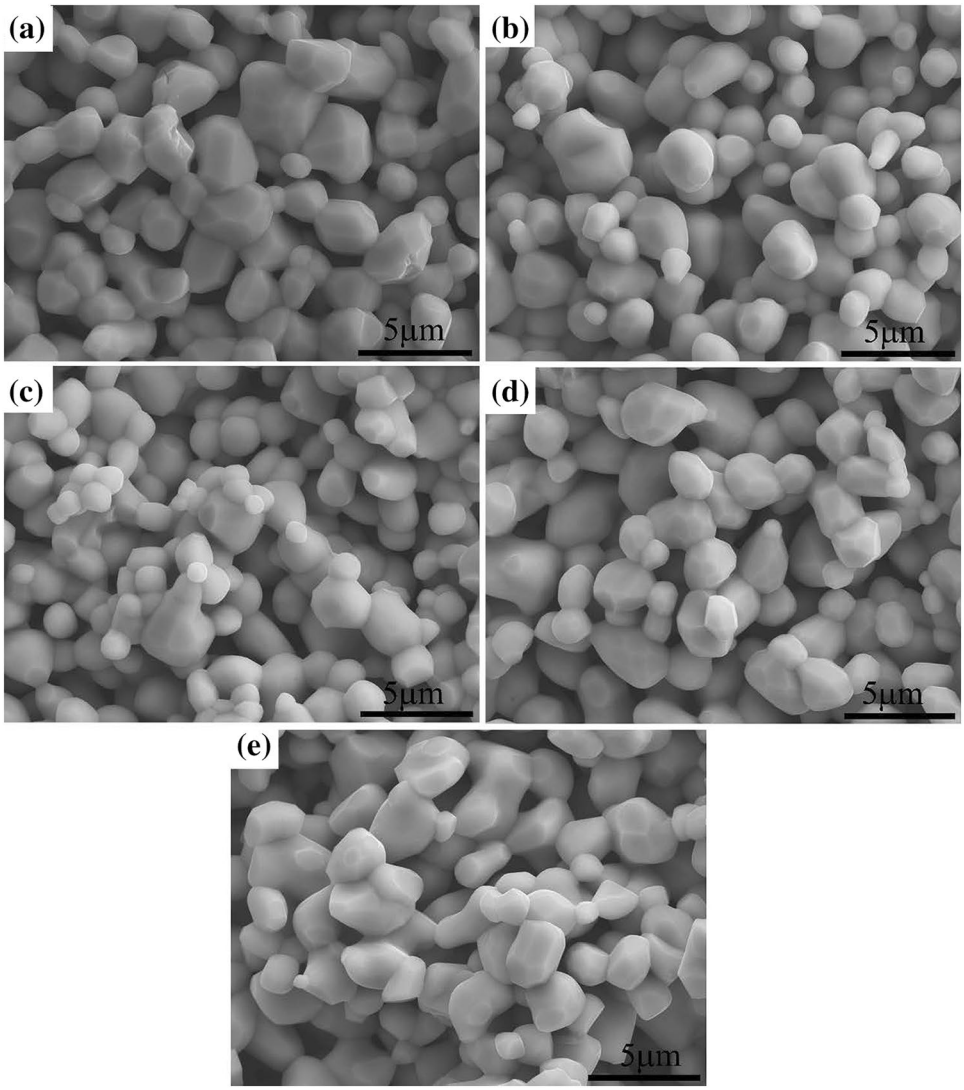

Fig. 2 SEM micrographs of the $La_{1-x}Sr_xCrO_3$ ceramics: **a** $x = 0$, **b** $x = 0.01$, **c** $x = 0.02$, **d** $x = 0.05$, **e** $x = 0.1$

where ρ is the resistance at infinite temperature, E_a is the activation energy, K is the Boltzmann constant and T is the absolute temperature. E_a can be calculated from the slope of the In ρ versus 1/T plots. It is also noted that the relationship between ln ρ and 1/T of all the samples turned out to be linear from Fig. 6. This linear dependence indicates an electrical conduction phenomena explained by polarons jumps [24]. The chromium volatilization at the high temperature in air atmosphere lead to the formation of Cr^{6+} ions. Due to the presence of these higher valent cations, holes are generated as per the following defect reaction [25]:

$$Cr^{3+} + 3h^{\cdot} \rightarrow Cr^{6+} \quad (2)$$

The holes, generated from the above equation, along with the lattice interaction form small polarons. In the present study, it not create any additional defect in $LaCrO_3$ ceramics, and therefore the conductivity is due to the polarons generated from Eq. (2). When $0.01 \leq x \leq 0.1$, for the substitution of La^{3+} by Sr^{2+}, the valence state of Cr^{3+} ions partially oxidized to Cr^{6+} to maintain the electrical neutrality. The ratio of Cr^{6+} to Cr^{3+} increases with x, this lead to the decrease in resistivity of $La_{1-x}Sr_xCrO_3$ system [17, 26] as the concentration of small polarons increases. This is agreement with the previous XPS results. As shown in Table 1, the values of ρ_{-70}, ρ_{-10}, $B_{-70/-10}$ constant and activation energy Eα of the thermistors were in the range of 16.51–84100, 4.77–2170 Ωcm, 1106–3268 K, and

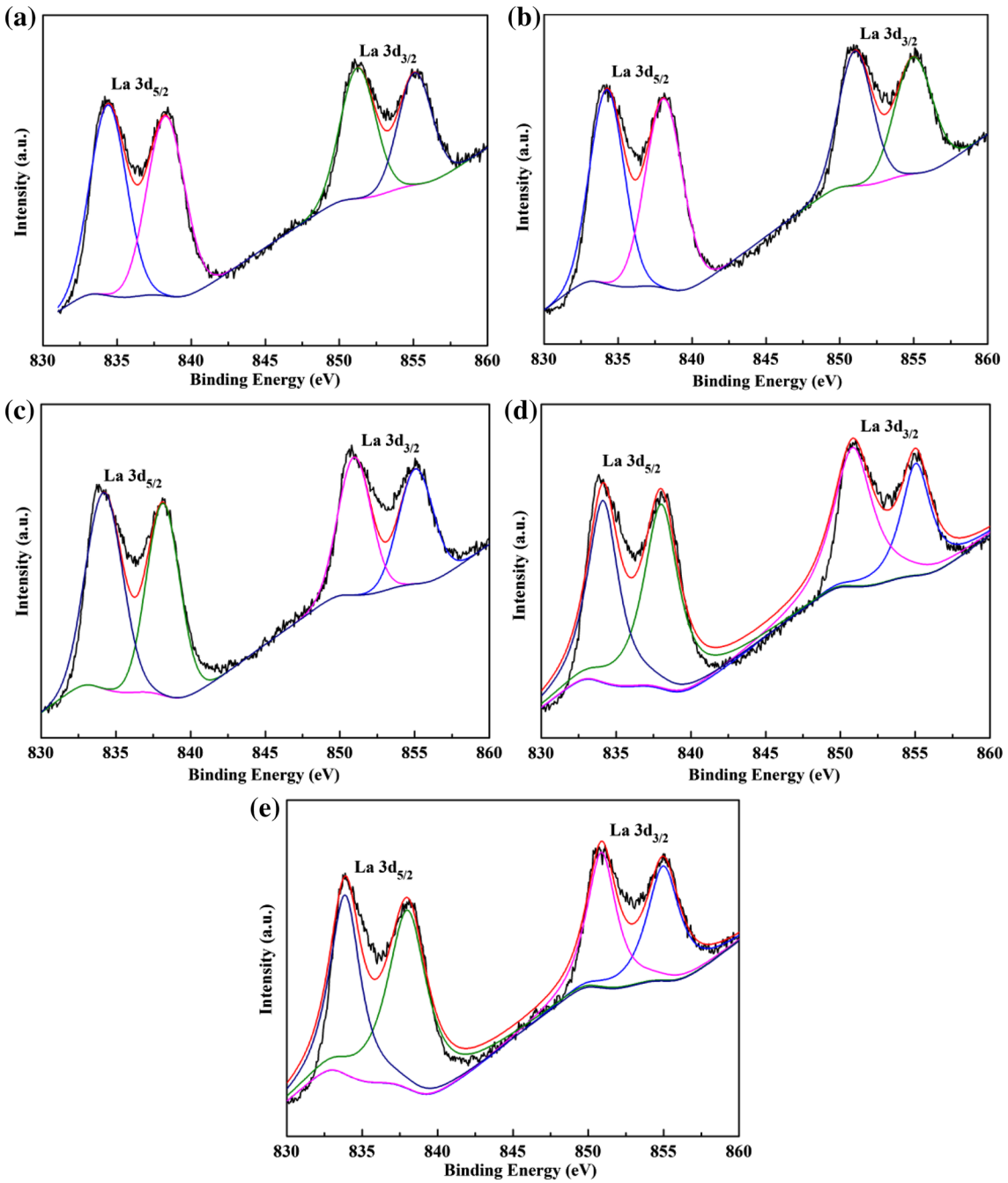

Fig. 3 La 3*d* XPS spectra collected for $La_{1-x}Sr_xCrO_3$ ceramics: **a** $x = 0$, **b** $x = 0.01$, **c** $x = 0.02$, **d** $x = 0.05$, **e** $x = 0.1$

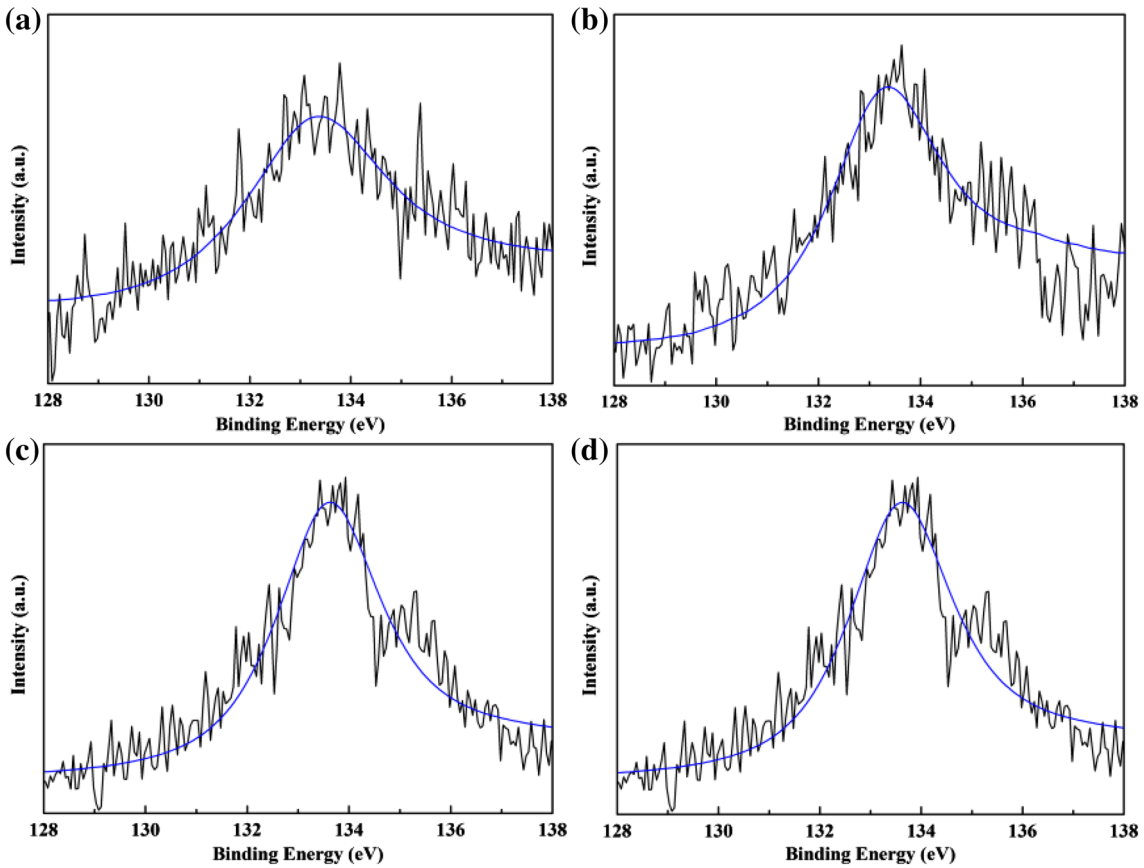

Fig. 4 Sr 3*d* XPS spectra collected for $La_{1-x}Sr_xCrO_3$ ceramics: **a** $x = 0.01$, **b** $x = 0.02$, **c** $x = 0.05$, **d** $x = 0.1$

0.095–0.283 eV, respectively. The *B* value can be calculated by the following equation [12]:

$$B = \left[\frac{T_1 T_2}{T_2 - T_1}\right] ln\left(\frac{R_1}{R_2}\right) \quad (3)$$

where R_1 and R_2 are the resistance value that measured by the temperature at T_1 and T_2, respectively. From Table 1 and Fig. 6 the variation trend of activation energy for different compositions of $La_{1-x}Sr_xCrO_3$ indicates that activation energy continuously decreases with Sr^{2+} ions increases. These results indicate that the electrical properties can be adjusted by the Sr^{2+} ions content.

In order to reveal the relation between ρ_{-70}, $B_{-70/-10}$ and Sr ions content clearly, Fig. 7 is presented. As shown in Fig. 7, the two lines have similar shapes, these results indicate that ρ_{-70} and $B_{-70/-10}$ of $La_{1-x}Sr_xCrO_3$ ceramics have the same tendency to increase of Sr^{2+} ions content.

4 Conclusions

The structure and electrical properties of $La_{1-x}Sr_xCrO_3$ ceramics has been investigated. The sintered ceramic samples are a single orthorhombic perovskite phase. The electrical conductivity in these ceramics is due to the polarons jumps between different oxidation states of chromium ions. The resistivity decreases with the increase of Sr^{2+} content, which is attributed to the increase of Cr^{6+}. The values of ρ_{-70}, ρ_{-10}, $B_{-70/-10}$ constant and activation energy Ea of the thermistors are in the range of 16.51–84100, 4.77–2170 Ωcm, 1106–3268 K, and 0.095–0.283 eV, respectively. The electrical properties can be adjusted by adjusting the Sr^{2+} concentration. These compounds could be used as potential candidates for NTC thermistors.

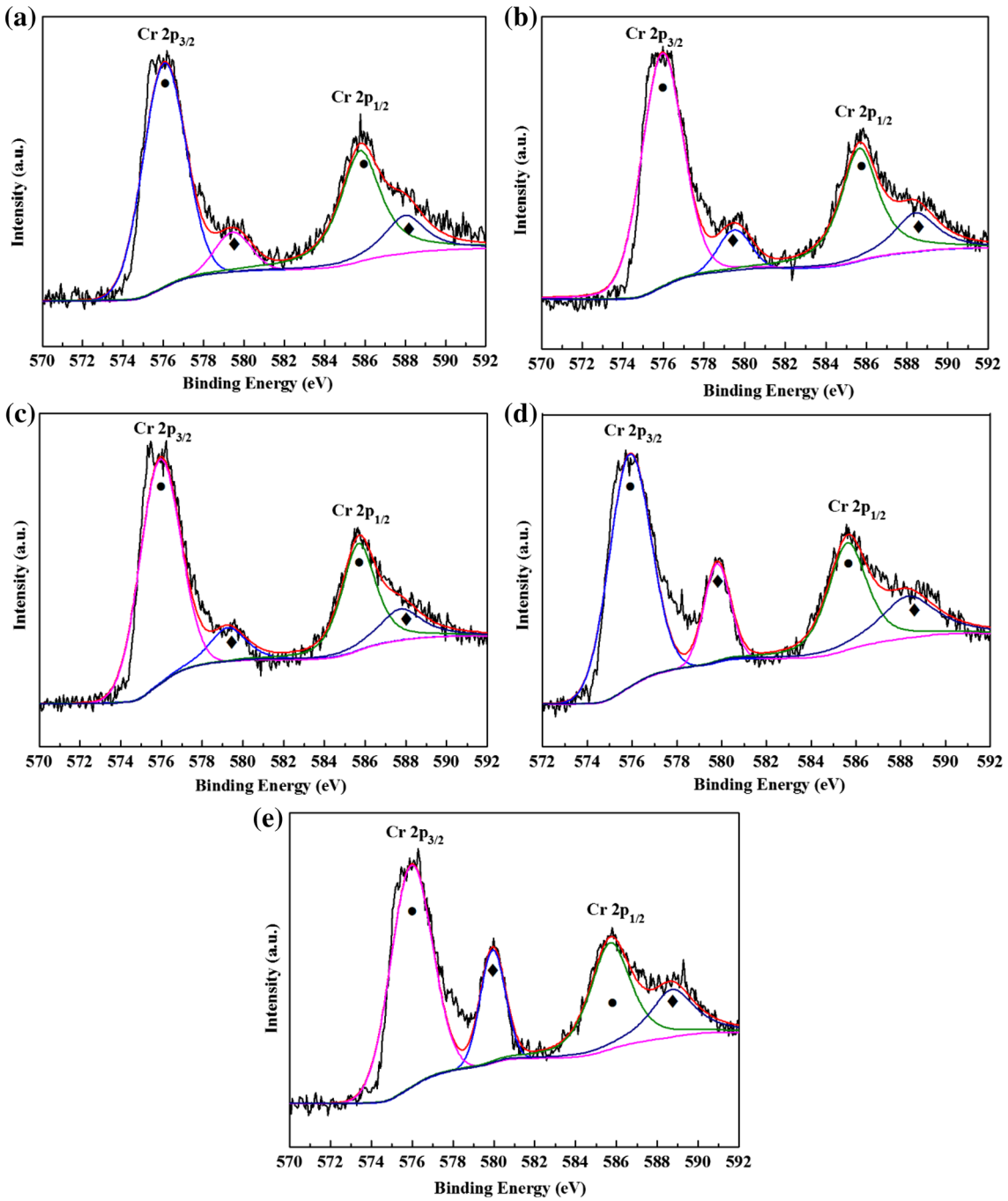

Fig. 5 XPS spectra results showing the Cr 2*p* regions of $La_{1-x}Sr_xCrO_3$ ceramics: **a** $x = 0$, **b** $x = 0.01$, **c** $x = 0.02$, **d** $x = 0.05$, **e** $x = 0.1$. *Filled circle* and *filled diamond* indicate the peaks of the Cr 2*p* spectra attributed to Cr^{3+} and Cr^{6+}, respectively

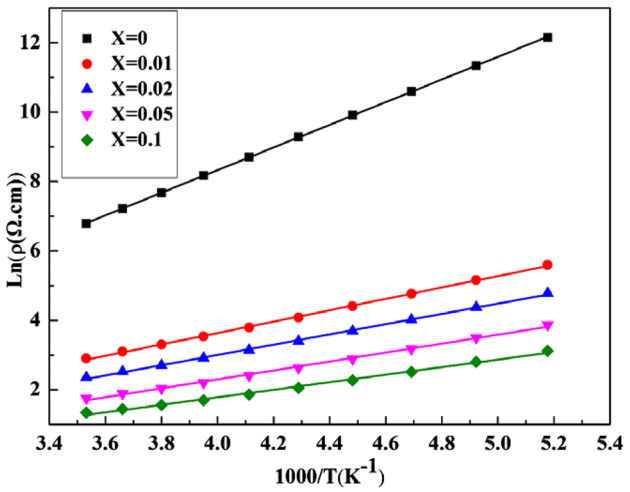

Fig. 6 Relationship between In ρ and 1000/T (k^{-1}) for the sintered sample corresponding for various compositions $La_{1-x}Sr_xCrO_3$

Table 1 ρ_{-70}, ρ_{-10}, $B_{-70/-10}$ constant and activation energy for the $La_{1-x}Sr_xCrO_3$ ceramics

x	ρ_{-70} (Ωcm)	ρ_{-10} (Ωcm)	$B_{-70/-10}$ (K)	E_a (eV)
0	8.41×10^4	2.17×10^3	3268	0.282
0.01	1.74×10^2	27.13	1653	0.142
0.02	80.05	14.98	1493	0.129
0.05	33.27	7.68	1306	0.113
0.1	16.51	4.77	1106	0.095

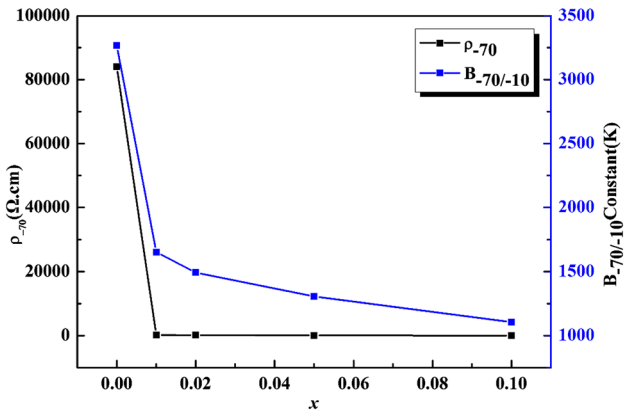

Fig. 7 Evolution of ρ_{-70} and $B_{-70/-10}$ constants as a function of Sr composition (x) for the sintered pellets

Acknowledgements This study was supported by the National Natural Science Foundation of China (Grant Nos. 61671447, 51502335), the Innovation Fund of Chinese Academy of Sciences (Grant No. CXJJ-15M047), and the West Light Foundation of the Chinese Academy of Sciences (Grant No. 2015-XBQN-B-13).

References

1. R. Koc, H.U. Anderson, J. Mater. Sci. **27**, 5477 (1992)
2. V.V. Kharton, A.P. Viskup, E.N. Naumovich, N.M. Lapchuk, Solid State Ion. **104**, 67 (1997)
3. Y. Jiang, J. Gao, M. Liu, Y. Wang, G. Meng, Mater. Lett. **61**, 1908 (2007)
4. M. Panneerselvam, K.J. Rao, J. Mater. Chem. **13**, 596 (2003)
5. D.H. Peck, M. Miller, D. Kobertz, H. Nickel, K. Hilpert, J. Am. Ceram. Soc. **79**, 3266 (1996)
6. N. Sakai, T. Kawada, H. Yokokawa, M. Dokiya, T. Iwata, J. Mater. Sci. **25**, 4531 (1990)
7. I. Yasuda, T. Hikita, J. Electron. Soc. **140**, 1699 (1993)
8. S.P. Jiang, L. Liu, K.P. Ong, P. Wu, J. Li, J. Pu, J. Power. Sour. **176**, 82 (2008)
9. S. Hayashi, K. Fukaya, H. Saito, J. Mater Sci. Lett. **7**, 457 (1988)
10. W.J. Weber, H.L. Tuller, T.O. Mason, A.N. Cormack, Mater. Sci. Eng. B **18**, 52 (1993)
11. A. Feteira, K. Reichmann, Adv. Sci. Technol. **67**, 124 (2010)
12. A. Feteira, J. Am. Ceram. Soc. **92**, 967 (2009)
13. X. Liu, W. Su, Z. Lu, J. Phys. Chem. Solids **62**, 1919 (2001)
14. H. Qi, Y. Luan, S. Che, L. Zuo, X. Zhao, C. Hou, Inorg. Chem. Commun. **66**, 33 (2016)
15. S.R. Nair, R.D. Purohit, A.K. Tyagi, P.K. Sinha, B.P. Sharma, J. Am. Ceram. Soc. **91**, 88 (2008)
16. H. Jiao, J. Wang, J. Ge, L. Zhang, H. Zhu, S. Jiao, Solid State Commun. **231**, 53 (2016)
17. X.N. Liu, W.H. Su, Z. Lu, J. Liu, L. Pei, W. Liu, L.Y. He, J. Alloy. Compd. **305**, 21 (2000)
18. H. Yokokawa, N. Sakai, T. Kawada, M. Kokiya, J. Electron. Soc. **138**, 1018 (1991)
19. H. Berthou, C.K. Jørgensen, C. Bonnelle, Chem. Phys. Lett. **38**, 199 (1976)
20. H. Van Doveren, J.A.T.H. Verhoeven, J. Electron. Spectrosc. Relat. Phenom. **21**, 265 (1980)
21. L. Li, Q. Wei, Z. Kang, M. Rui, W. Su, J. Alloy. Compd. **249**, 264 (1997)
22. A.N. Kamlo, J. Bernard, C. Lelievre, D. Houivet, J. Eur. Ceram. Soc. **31**, 1457 (2011)
23. M.A.L. Nobre, S. Lanfredi, Appl. Phys. Lett. **81**, 451 (2002)
24. B. Zhang, Q. Zhao, A. Chang, H. Yan, Y. Wu, J. Mater. Sci. Mater. Electron. **24**, 4452 (2013)
25. A.K. Tripathi, H.B. Lal, J. Mater. Sci. **17**, 1595 (1982)
26. W.J. Weber, C.W. Griffin, J.L. Bates, J. Am. Ceram. Soc. **70**, 265 (1987)